

# Kinetic dynamo in non-magnetized plasmas impeded by magnetic Landau damping

I. Pusztai<sup>1</sup>, J. Juno<sup>2</sup>, A. Brandenburg<sup>3</sup>, J. M. TenBarge<sup>4,5</sup>, A. Hakim<sup>5</sup>, M. Francisquez<sup>6</sup>,  
and A. Sundström<sup>1</sup>

<sup>1</sup> Department of Physics, Chalmers University of Technology, Göteborg, Sweden

<sup>2</sup> Department of Physics and Astronomy, University of Iowa, Iowa City, IA 54224, USA

<sup>3</sup> NORDITA, KTH Royal Inst. Technology and Stockholm University, SE-10691 Stockholm, Sweden

<sup>4</sup> Department of Astrophysical Sciences, Princeton University, Princeton, NJ 08544, USA

<sup>5</sup> Princeton Plasma Physics Laboratory, Princeton, NJ 08540, USA

<sup>6</sup> Plasma Science and Fusion Center, Massachusetts Inst. of Technology, Cambridge, MA, 02139, USA

Observational evidence is consistent with the generation and maintenance of the magnetic fields permeating the Universe being caused by turbulent dynamo. Galaxy clusters are weakly collisional on scales relevant for the dynamo process. However, due to the computational challenges related to the inherently three-dimensional and multiscale nature of dynamo, only a very few recent works have gone beyond an MHD description [1, 2], using a hybrid treatment.

We perform fully kinetic continuum simulations in an electron-proton plasma [3] of the Galloway-Proctor (GP) [4] flow, using the kinetic-Maxwell solver of `Gkeyll` [5], for parameters producing dynamo in magnetohydrodynamics (MHD), and complement these with collisionless fluid simulations using the 10-moment, two-fluid solver of `Gkeyll` [6]. We consider scenarios with low fluid Reynolds number and high magnetic Prandtl number and a non-magnetized initial condition, with relevance for galaxy clusters at typical seed field levels.

The kinetic-Maxwell solver of `Gkeyll` solves the kinetic equation  $\partial_t f_a + \mathbf{v} \cdot \nabla f_a + \mathbf{a}_a \cdot \nabla_{\mathbf{v}} f_a = C[f_a]$ , for all species  $a$ , with mass  $m_a$ , charge  $e_a$ , and distribution function  $f_a$ . In the acceleration term,  $\mathbf{a}_a = \mathbf{f}_a/m_a + (e_a/m_a)(\mathbf{E} + \mathbf{v} \times \mathbf{B})$ , the electric and magnetic fields,  $\mathbf{E}$  and  $\mathbf{B}$ , are computed from Maxwell's inductive equations, and  $\mathbf{f}_a(\mathbf{x}, t)$  is an externally prescribed forcing. Collisions are modeled by a conservative Dougherty operator [7],  $C[f_a]$ . The simulations are initialized with Maxwellian electrons ( $e$ ) and protons ( $i$ ), with temperature  $T_a = 1\text{ keV}$ , density  $n_a = 2.3 \times 10^{28} \text{ m}^{-3}$ , and a flow with a characteristic speed  $u_0 = M_0 \sqrt{T_e/m_i}$  and  $M_0 = 0.35$ . These parameters give a magnetic Reynolds number  $\text{Rm} \approx 13$  (for Spitzer resistivity), a magnetic Prandtl number  $\text{Pm} \approx 20$  (for collisional viscosity), and a collisional mean free path  $\lambda = 1.25 \mu\text{m}$ , for a box size (flow forcing scale) of  $L_0 = 9.73 \mu\text{m}$  and an assumed  $\ln \Lambda = 10$ .

We consider the GP flow that produces a fast dynamo and requires a low critical  $\text{Rm}$ ,

$$\mathbf{u}_{\text{GP}}(\mathbf{x}, t) = u_0 \{ \sin(k_0 z + \sin \omega t) + \cos(k_0 y + \cos \omega t), \cos(k_0 z + \sin \omega t), \sin(k_0 y + \cos \omega t) \},$$

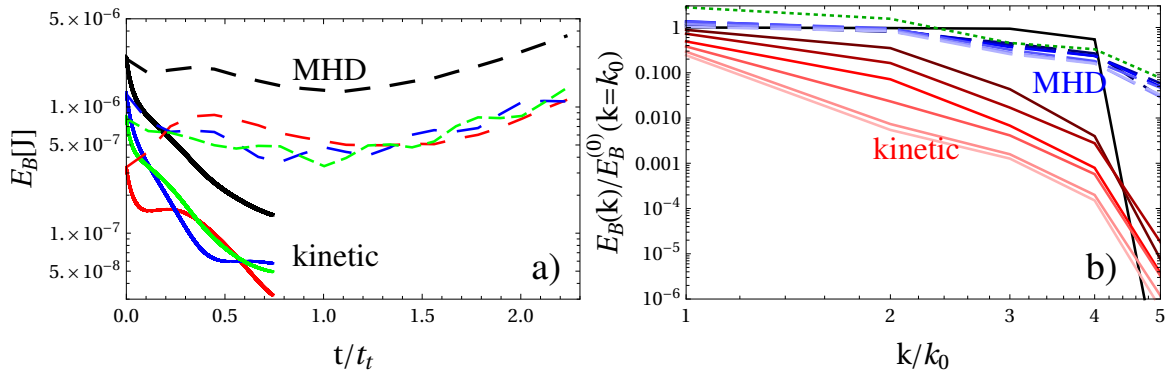


Figure 1: **a)** Volume integrated magnetic energy. Solid lines: kinetic simulation; dashed: resistive MHD. Red, blue, and green correspond to the contributions from  $x$ ,  $y$ , and  $z$  field components to the total (black). For reference,  $(3/2)n_i T_i L_0^3 = 5.1 \times 10^{-3}$  J. **b)** Wave number spectra of magnetic energy,  $E_B(k)$  (normalized to its value at  $k_0$ ,  $t = 0$ ), for  $t = \{0, 1, 2, \dots, 6\} \times 10^{-11}$  s (lines lightening). Solid lines: kinetic simulation; dashed: MHD; dotted line: MHD in the growing phase  $t = 2 \times 10^{-10}$  s. Figures reproduced from [3].

where  $k_0 = 2\pi/L_0$ ,  $\omega = 2\pi/t_t$ , and  $t_t = L_0/u_0 \approx 9 \times 10^{-11}$  s is the turnover time. The flow is sustained by exerting a force of  $\mathbf{f}_i = C_f m_i \mathbf{u}(\mathbf{x}, t)/t_i$  on the ions, with the thermal ion passing time  $t_i = L_0/\sqrt{2T_i/m_i}$ ; we set  $C_f = 1$ . The initial magnetic field is  $B_0 \sum_{j \neq i, n} b_{ij,n} \cos[nk(x_i + \varphi_{ij,n})]$ , where  $b_{ij,n}$  and  $\varphi_{ij,n}$  are uniform random numbers on  $[0, 1]$ ,  $n = 1, 2, \dots, N$  with  $N = 4$ , and  $B_0 = 40$  T (the thermal electron gyro-radius is  $2.7 \mu\text{m}$ ). In addition to  $\mathbf{u}_{\text{GP}}$ , the initial electron flow also has a component producing a current consistent with the magnetic seed field.

The value  $\text{Rm} \approx 13$  is sufficient for the GP flow to produce magnetic field growth in resistive MHD, as confirmed using the high order finite-difference MHD solver Pencil Code [8]. We find that, after a slight decay, the magnetic field starts to grow exponentially, as shown in Fig. 1a (dashed). However, in the kinetic simulation, the field energy is observed to monotonically decay (solid). The magnetic energy in the kinetic simulation rapidly develops a strongly decaying wave number spectrum (solid lines in Fig. 1b), defined such that  $E_B = \int E_B(k) dk$ . In contrast, the spectrum corresponding to the MHD simulation quickly assumes its weakly decaying shape (dashed), which is then preserved in the phase of exponential growth (dotted).

The decay of the magnetic field energy in the kinetic simulation is caused by Landau damping of the magnetic fluctuations. For an elementary magnetic perturbation  $B_z(x, t = 0) = B_0 \cos(kx)$ , resistive magnetic diffusion  $\partial_t \mathbf{B} = \eta \nabla^2 \mathbf{B}$  leads to a decay  $B_z \propto \exp(-\gamma t) = \exp(-k^2 \eta t)$ . In a weakly collisional plasma, i.e.,  $\nu_{ei} \rightarrow +0$ , where  $\nu_{ei}$  is the electron-ion collision frequency, such a fluctuation decays due to Landau damping with a decay rate  $\gamma = |k|^3 c^2 v_e / (\sqrt{\pi} \omega_{pe}^2) = |k|^3 v_e m_e / (\sqrt{\pi} \mu_0 n_e e^2)$  [9], where  $\omega_{pe} = \sqrt{n_e e^2 / (\epsilon_0 m_e)}$ ,  $v_e = \sqrt{2T_e/m_e}$  is the electron thermal

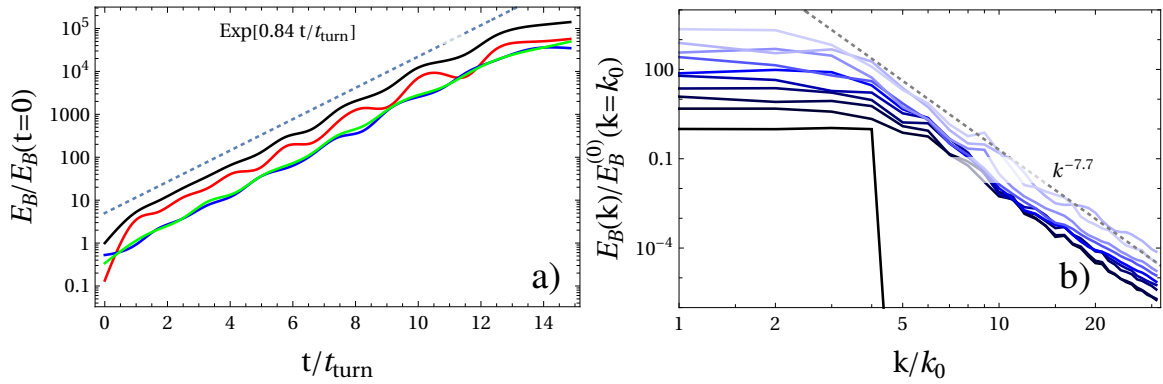


Figure 2: a) Magnetic energy normalized to its initial value in a collisionless fluid simulation. Red, blue, and green correspond to the contributions from  $x$ ,  $y$ , and  $z$  field components to the total (black). Dotted:  $e^{0.84t/t_{\text{turn}}}$ . b) Wave number spectra of magnetic energy,  $E_B(k)$  (normalized to its value at  $k_0$ ,  $t = 0$ ), for  $t/t_{\text{turn}} = 0.825 \times \{0, 1, \dots, 9\}$ , (lines lightening). Dotted:  $k^{-7.7}$ .

speed,  $-e$  and  $n_e$  are the electron charge and density, and  $\epsilon_0$  denotes the vacuum permittivity. We would get this decay rate from resistive diffusion, if we replaced  $\sigma^{-1}$  with a scale-dependent effective resistivity  $\sigma_{\text{eff}}^{-1} = |k|v_e m_e/(\sqrt{\pi} n_e e^2)$ , which corresponds to an effective magnetic diffusivity  $\eta_{\text{eff}} \sim \eta \lambda/l$ , where  $\lambda = v_e/\nu_{ei}$  is the Coulomb mean free path, and  $2\pi/l = |k|$ .

Kinetic Gkeyll simulations reproduce the above damping rate in the collisionless limit, as well as the decay rate corresponding to a magnetic diffusion due to Spitzer resistivity in the short mean free path limit. When the collision frequency is increased from the collisionless limit, the free streaming required by the Landau damping gets interrupted by collisions, leading to a reduction of the damping rate, before magnetic diffusion takes over at even higher collisionalities. Thus, the damping rate assumes a minimum at intermediate collisionalities. We have also confirmed that the Landau damping of magnetic perturbations diminishes as the plasma gets magnetized and the gyro-radius becomes smaller than the scale of the perturbations.

When electrons are not magnetized down to the resistive scale  $l_\eta$ , the cutoff of the magnetic energy spectrum is expected to be located at a scale where the growth of magnetic perturbations—due to stretching at the viscous scale,  $l_\nu$ —is balanced by Landau damping. The ratio of this *Landau scale* and  $l_\nu$  is found to be  $l_L/l_\nu \sim M_0^{1/3} \text{Re}^{-1/12} \text{Pm}^{-1/3}$  in asymptotically scale separated systems, where  $M_0$  is the Mach number at the outer scale and  $\text{Re}$  is the fluid Reynolds number. While  $M_0$  and  $\text{Re}$  are not very different to unity in galaxy cluster plasmas,  $\text{Pm} \gg 1$ , thus  $l_L \gg l_\eta$ , i.e., the cutoff scale of magnetic perturbations is larger than in resistive MHD.

While fully kinetic simulations become extremely expensive with a spatial resolution suitable to capture the shrinking gyro-radius in a magnetized electron simulation with magnetic field growth, the 10-moment collisionless fluid model of Gkeyll allows the exploration of such

parameter regimes. It evolves the full pressure tensor of both particle species, allowing the electron viscous stress to balance the induced electric field, which is a key mechanism in the Landau damping of magnetic perturbations. As the field lines are stretched, folded and compressed by the flow, without collisions or small-scale instabilities, the pressure anisotropy is expected to grow without bounds, while the dynamo is unable to amplify the total field energy. Here, we employ a closure that independently isotropizes the pressure for each species [10],  $\partial_m Q_{ijm} = (v_t/l_{\text{iso}})(P_{ij} - p\delta_{ij})$ , where  $Q_{ijm}$  and  $P_{ij}$  are the heat flux tensor and the pressure tensor,  $v_t$  is the thermal speed of the species, and  $l_{\text{iso}}$  is a parameter of dimension length which sets the strength of the isotropization. We observe that increasing  $l_{\text{iso}}$  for electrons (ions) leads to a stronger decay of the magnetic field (flow velocities) in simulations with no flows (no forcing of flows). Thus, these parameters may be used to emulate systems with different effective magnetic and fluid Reynolds numbers.

We use parameters similar to the kinetic simulation above, except that we use a reduced ion mass  $m_i^{\text{red}} = 100m_e$ , a box size of  $L_0 = 24.3\mu\text{m}$ , a forcing factor  $C_f = 2.5$ , and a seed field amplitude  $B_0 = 1\text{ T}$  (initially electrons are unmagnetized). To introduce dissipation in a system with no explicit collisions, we set  $l_{\text{iso}} = L_0/1280$  for electrons and  $L_0/12.8$ , corresponding to a high effective magnetic Prandtl number. For these parameters, we find an approximately exponential magnetic energy growth—with no significant change in the growth rate as the electrons become magnetized—see Fig. 2a, which continues 5 decades before the smallest thermal electron Larmor radius reaches grid scale ( $L_0/128$ ). The magnetic energy in the box undergoes increasing oscillations superimposed on the growth. The magnetic energy spectrum, shown in Fig. 2a, is flat up to  $k/k_0 \sim 4$ , above which it decreases with a very strong exponent, approximately as  $k^{-7.7}$ . The flow energy spectrum (not shown here) is  $k^{-5}$  and steeper for  $k/k_0 > 10$ .

**Conclusions** In magnetized high-Pm systems, such as galaxy clusters, the collisionless scales are believed to be important for turbulent dynamo. However, at typical seed magnetic field levels collisionless scales are unmagnetized, allowing Landau damping of magnetic perturbations to impede the dynamo. The cutoff-scale of magnetic perturbations is then larger than the resistive scale. Collisionless fluid models with appropriate closures can help explore this regime.

## References

- [1] F Rincon et al. PNAS **113**, 3950 (2016).
- [2] DA St-Onge et al. ApJ **863**, l25 (2018).
- [3] I Pusztai et al. PRL **124**, 255102 (2020).
- [4] DJ Galloway et al. Nature **356**, 691 (1992).
- [5] J Juno et al. JCP **353**, 110 (2018).
- [6] L Wang et al. JCP **415**, 109510 (2020).
- [7] A Hakim et al. JPP **86**, 905860403 (2020).
- [8] <http://pencil-code.nordita.org>
- [9] AB Mikhailovskii, Plasma Phys **22**, 133 (1980)
- [10] L Wang et al. PoP **22**, 012108 (2015).